Figure S1

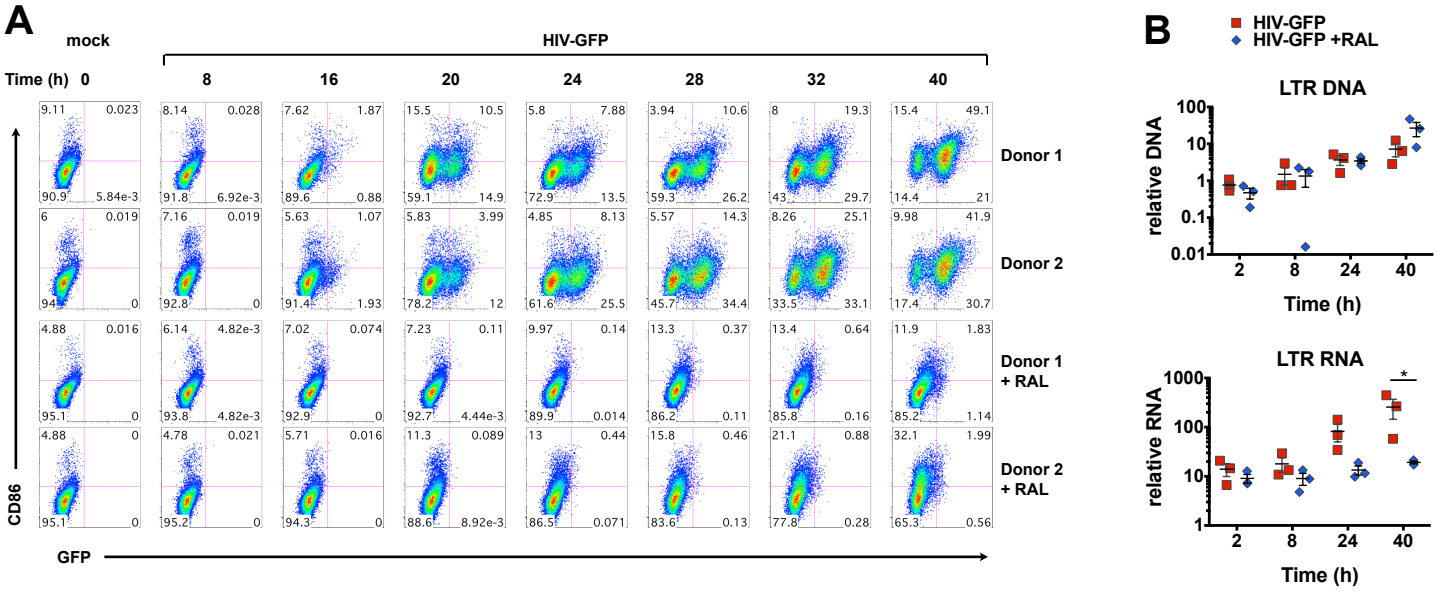
A
mock
HIV-GFP
Time (h) 0 8 16 20 24 28 32 40
Donor 1
Donor 2
Donor 1 + RAL
Donor 2 + RAL
CD86
GFP
B
HIV-GFP
HIV-GFP +RAL
LTR DNA
relative DNA
Time (h)
LTR RNA
relative RNA
Time (h)

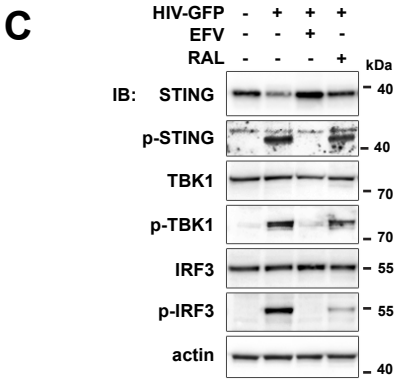
C
HIV-GFP
EFV
RAL
kDa
IB: STING
p-STING
TBK1
p-TBK1
IRF3
p-IRF3
actin

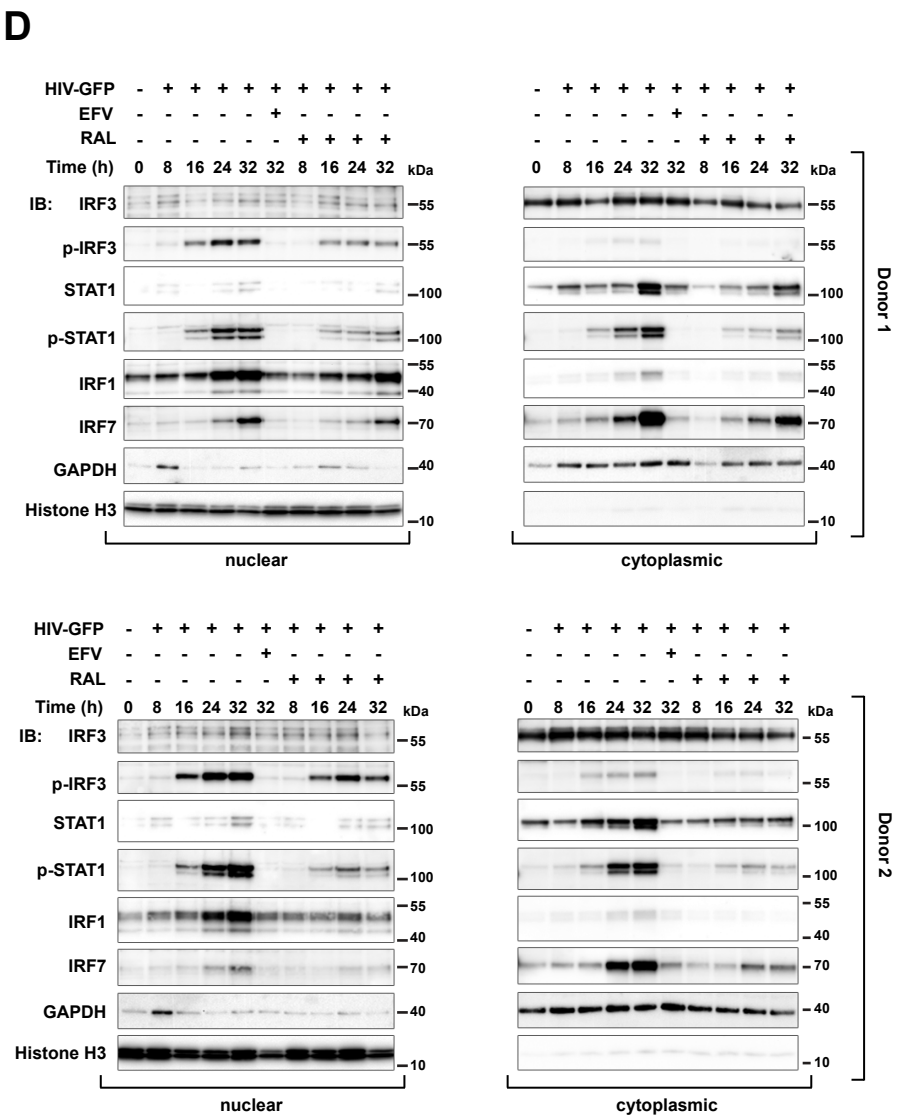
D
HIV-GFP
EFV
RAL
Time (h) 0 8 16 24 32 32 8 16 24 32
kDa
IB: IRF3
p-IRF3
STAT1
p-STAT1
IRF1
IRF7
GAPDH
Histone H3
nuclear
cytoplasmic
Donor 1
Donor 2

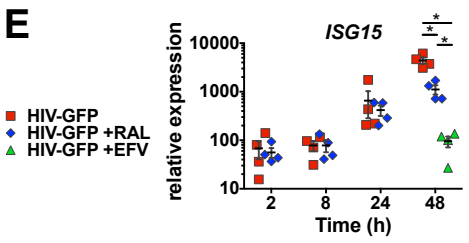
E
HIV-GFP
HIV-GFP +RAL
HIV-GFP +EFV
ISG15
relative expression
Time (h)

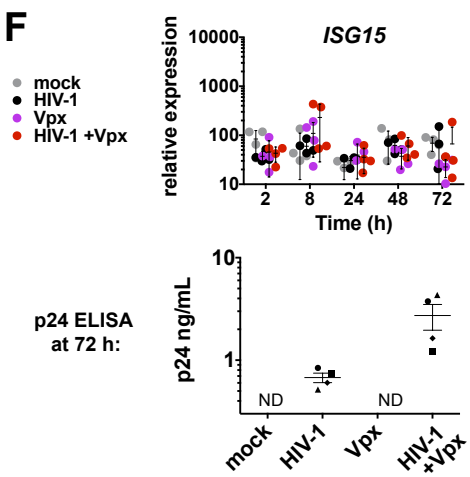
F
mock
HIV-1
Vpx
HIV-1 +Vpx
ISG15
relative expression
Time (h)
p24 ELISA at 72 h:
p24 ng/mL
ND
ND
mock
HIV-1
Vpx
HIV-1 +Vpx

Figure S1. Pre-integration sensing coincides with phosphorylation of IRF3 and occurs prior to early reporter expression during HIV-GFP infection. Related to Figure 1.

(A) Flow cytometry plots of CD86 vs GFP expression in DCs after infection with HIV-GFP +/- RAL for the indicated times. (MOI = 1.5)

(B) qPCR of accumulating HIV-1 DNA and RNA during infection in DCs +/- RAL. n = 3 donors.

(C) Immunoblots of whole cell lysates 24 h after infection with HIV-GFP +/- RAL or EFV. Phospho-specific antibodies detect phosphorylated S366 for STING, S172 for pTBK1, and S396 for IRF3.

(D) Immunoblots of nuclear/cytoplasmic fractionations of DCs treated for the indicated times in the presence or absence of RAL or EFV. Phospho-specific antibodies detect S396 for IRF3 and Y701 for STAT1. 10 μg of protein was loaded in each well and blots for nuclear and cytoplasmic fractions were developed under identical conditions for the antibodies shown. Under these conditions, the antibody used for detecting total IRF3 was less sensitive than anti-p-IRF3 when immunoblotting for IRF3 in the nuclear fraction, possibly due to masking of the epitope. GAPDH and Histone H3 serve as controls for fractionation of the cytoplasm and nucleus, respectively. The authors note that the appearance of GAPDH in the nuclear fraction for the 8 h HIV-GFP time point in samples from both donors shown could be a coincidental technical effect, as this was not observed in sample preparations of other donors.

(E) qPCR of *ISG15* expression during infection in DCs in the presence or absence of RAL and EFV. n = 4 donors.

(F) DCs at day 4 after differentiation were infected with replication competent CD4/CCR5-tropic HIV-1 (2.5 ng/ml p24) either with or without Vpx. DC media was replaced at day 1 and day 2 after infection. Data show ELISA of p24 concentration in DC supernatants at 72 h post inoculation and a time course of *ISG15* expression in matched donors. n = 4 donors.

Panels with pooled data show mean +/- SEM. See also Figure S1.

Figure S2

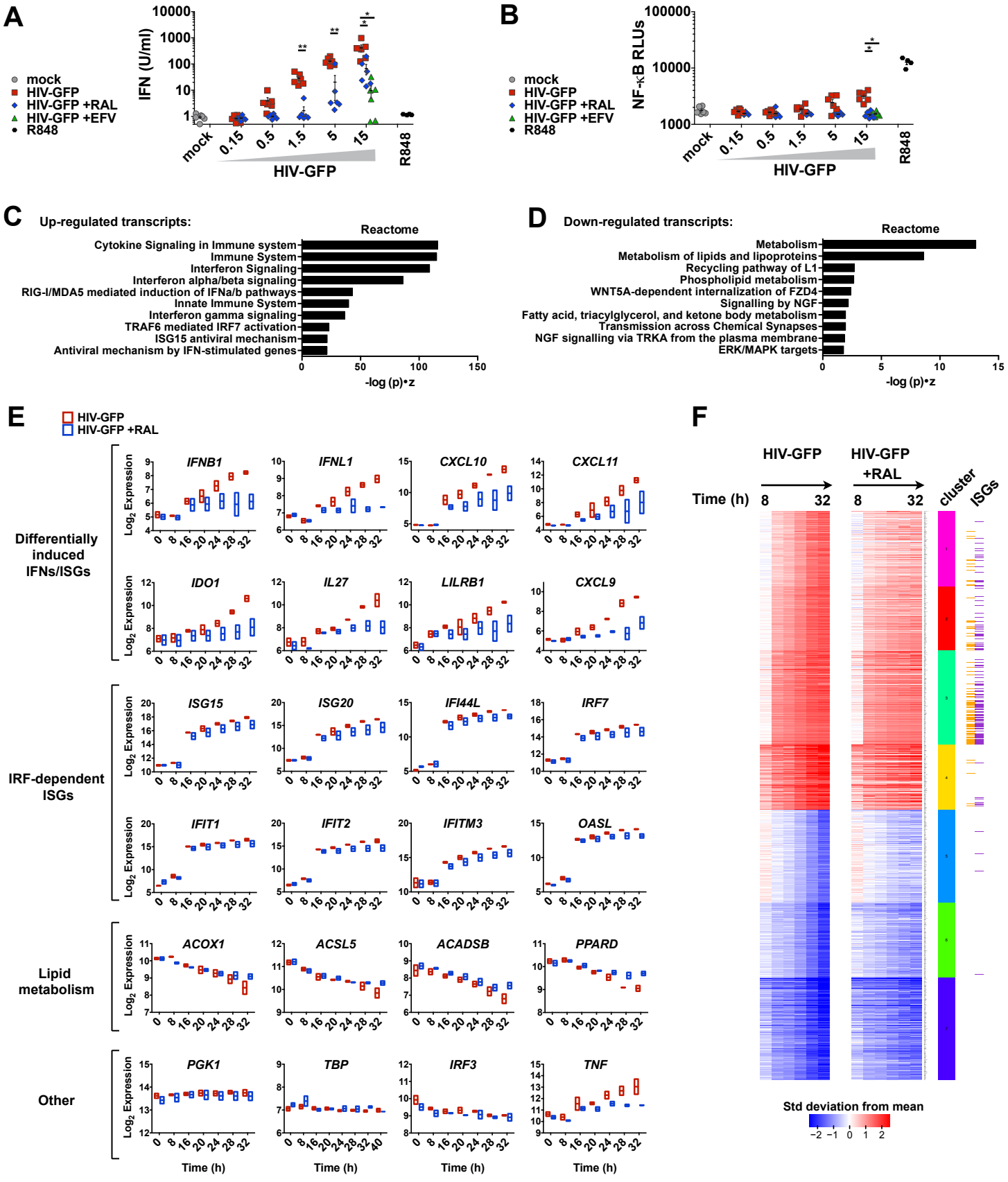
A
mock
HIV-GFP
HIV-GFP +RAL
HIV-GFP +EFV
R848
IFN (U/ml)
HIV-GFP
B
NF-κB RLUs
C
Up-regulated transcripts:
Reactome
Cytokine Signaling in Immune system
Immune System
Interferon Signaling
Interferon alpha/beta signaling
RIG-I/MDA5 mediated induction of IFNa/b pathways
Innate Immune System
Interferon gamma signaling
TRAF6 mediated IRF7 activation
ISG15 antiviral mechanism
Antiviral mechanism by IFN-stimulated genes
-log (p)•z
D
Down-regulated transcripts:
Metabolism
Metabolism of lipids and lipoproteins
Recycling pathway of L1
Phospholipid metabolism
WNT5A-dependent internalization of FZD4
Signalling by NGF
Fatty acid, triacylglycerol, and ketone body metabolism
Transmission across Chemical Synapses
NGF signalling via TRKA from the plasma membrane
ERK/MAPK targets
E
HIV-GFP
HIV-GFP +RAL
Differentially induced IFNs/ISGs
IRF-dependent ISGs
Lipid metabolism
Other
IFNB1
IFNL1
CXCL10
CXCL11
IDO1
IL27
LILRB1
CXCL9
ISG15
ISG20
IFI44L
IRF7
IFIT1
IFIT2
IFITM3
OASL
ACOX1
ACSL5
ACADSB
PPARD
PGK1
TBP
IRF3
TNF
Log2 Expression
Time (h)
F
HIV-GFP
HIV-GFP +RAL
Time (h)
cluster
ISGs
Std deviation from mean

Figure S2. IFNs and ISGs are induced to different degrees before and after HIV-1 integration. Related to Figure 2.

(A) Bioactive type I IFN and (B) NF-κB activity in supernatants from DCs exposed to increasing titers of HIV-GFP, HIV-GFP +RAL, HIV-GFP +EFV (n = 6 donors); or R848 as shown (n = 4 donors); mean +/- SEM.

(C) Reactome pathway analysis of up-regulated transcripts identified from a mixed model regression analysis (FDR < 0.01 and absolute log2 fold change > 1).

(D) Reactome pathway analysis of down-regulated transcripts identified as in (A).

(E) Array data plotted for individual genes in DCs during HIV-GFP infection +/- RAL over the depicted time course (IFNs and ISGs that are differentially induced, canonical IRF-dependent ISGs, genes involved in lipid metabolism that are repressed (*ACOX1, ACSL5, ACADSB, PPARD*), housekeeping genes (*PGK1, TBP*), and other genes implicated in the innate response (*IRF3, TNF*)). Boxes indicate mean and range of log2-normalized expression. n = 2 donors.

(F) Hierarchical Ordered Partitioning and Collapsing Hybrid (HOPACH) clustering of genes from microarray analysis. Heat maps are row-scaled with colors representing fold-change from mock-infected DCs. Hallmark IFN genes annotated by the Molecular Signatures Database, or classic ISGs (Schoggins et al. 2011) are denoted with orange or purple hash marks, respectively.

Figure S3

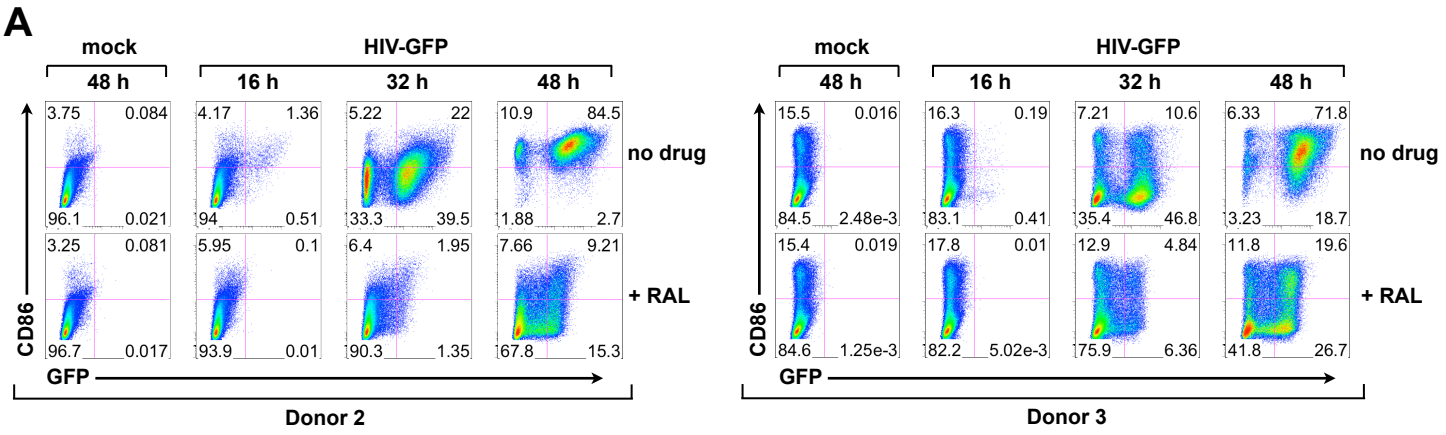
A
mock
HIV-GFP
48 h
16 h
32 h
48 h
no drug
+ RAL
CD86
GFP
Donor 2
Donor 3

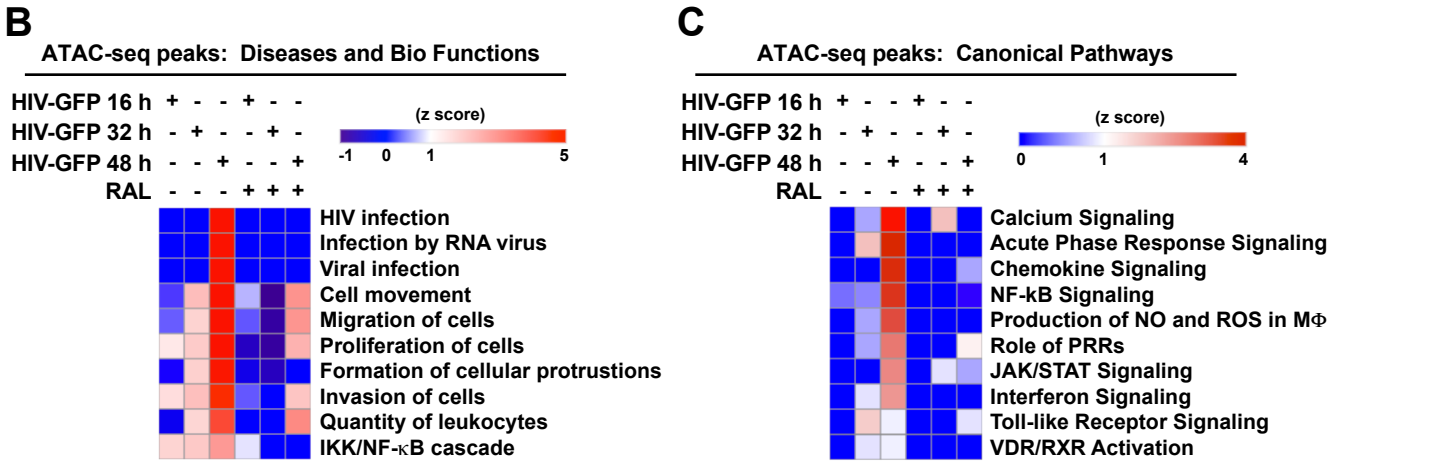
B
ATAC-seq peaks: Diseases and Bio Functions
HIV-GFP 16 h
HIV-GFP 32 h
HIV-GFP 48 h
RAL
(z score)
HIV infection
Infection by RNA virus
Viral infection
Cell movement
Migration of cells
Proliferation of cells
Formation of cellular protrustions
Invasion of cells
Quantity of leukocytes
IKK/NF-κB cascade
C
ATAC-seq peaks: Canonical Pathways
Calcium Signaling
Acute Phase Response Signaling
Chemokine Signaling
NF-kB Signaling
Production of NO and ROS in MΦ
Role of PRRs
JAK/STAT Signaling
Interferon Signaling
Toll-like Receptor Signaling
VDR/RXR Activation

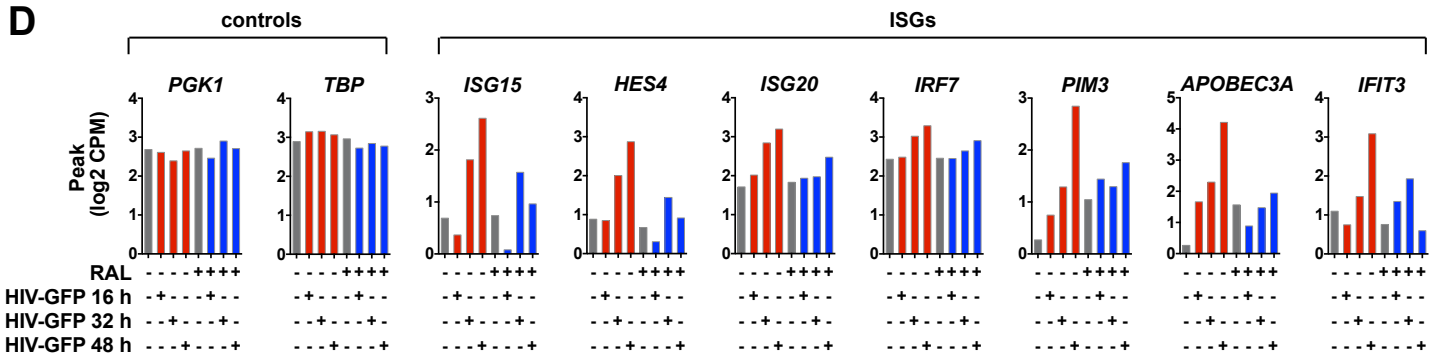
D
controls
ISGs
PGK1
TBP
ISG15
HES4
ISG20
IRF7
PIM3
APOBEC3A
IFIT3
Peak (log2 CPM)
RAL
HIV-GFP 16 h
HIV-GFP 32 h
HIV-GFP 48 h

Figure S3. Blocking integration suppresses HIV-mediated DC activation and open chromatin responses. Related to Figure 3.

(A) Flow cytometry of DCs from Donors 2 and 3 that were prepped for ATAC-seq. (Donor 1 is shown in Figure 6B). DC were infected with HIV-GFP in the presence of Vpx +/- RAL for 16, 32, or 48 h, with plots depicting CD86 vs GFP expression.

(B) Ingenuity Pathway Analysis software was used to identify likely Diseases and Biological Functions associated with open chromatin changes in HIV-infected DCs. Genes found in ATAC-seq peaks that were differentially accessible compared to mock ($p < 0.05$) were used for the analysis. Heat maps are displayed as z scores for the relevant Functions and Pathways. Rows were sorted from top to bottom based on scores for HIV-GFP analysis at 48 h.

(C) Canonical Pathways associated with differential open chromatin peaks identified from Ingenuity Pathway Analysis of ATAC-seq as in (B).

(D) ATAC-seq gene-associated peak values for the housekeeping genes PGK1 and TBP or the ISGs shown were graphed for the conditions from (A) as counts per million reads (CPM). Peaks for *APOBEC3A* and *IFIT3* were scaled by a factor of 3 in relation to other genes.

Figure S4

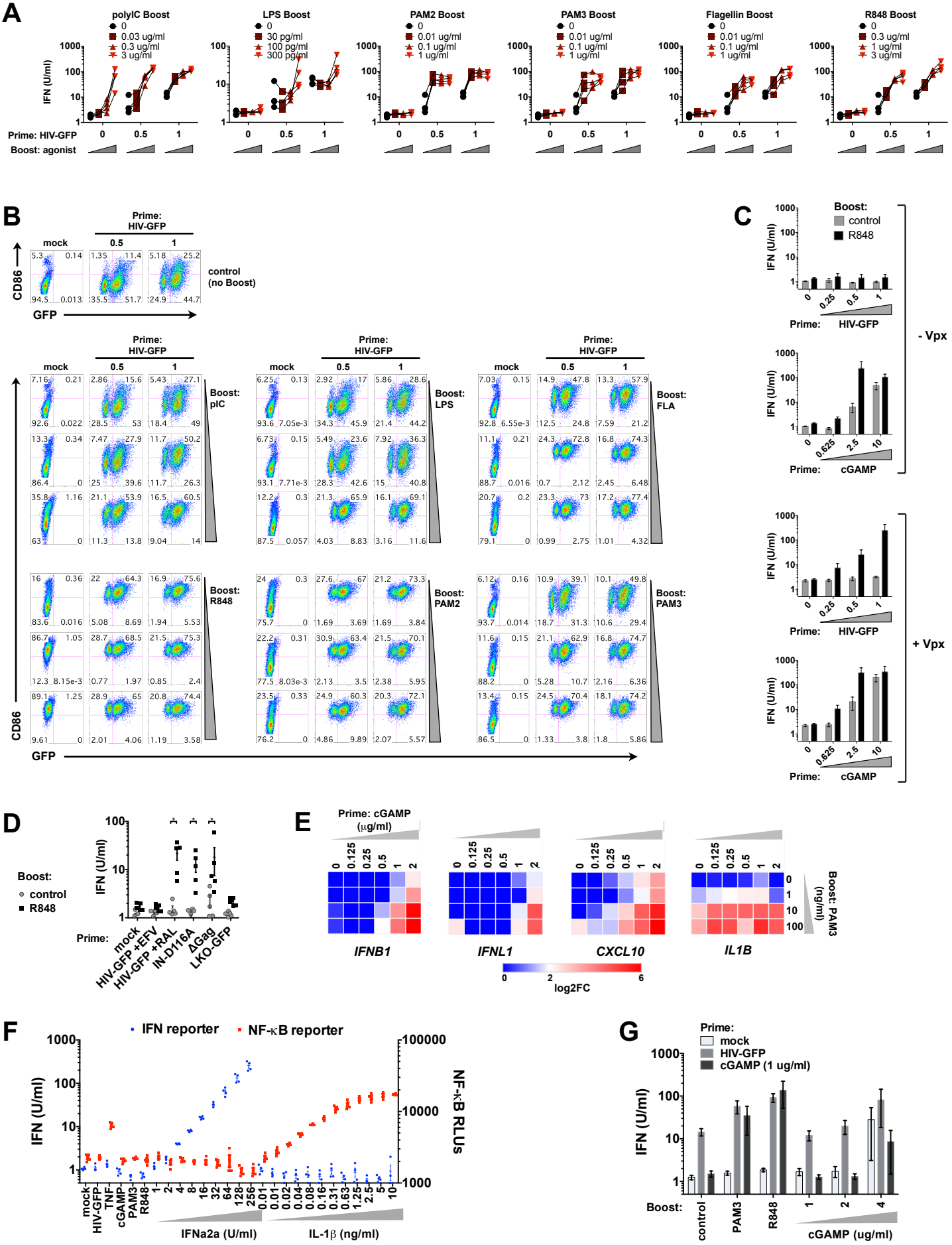
A
polyIC Boost
LPS Boost
PAM2 Boost
PAM3 Boost
Flagellin Boost
R848 Boost
IFN (U/ml)
Prime: HIV-GFP
Boost: agonist
B
Prime: HIV-GFP
mock
0.5
1
CD86
GFP
control (no Boost)
Boost: pIC
Boost: LPS
Boost: FLA
Boost: R848
Boost: PAM2
Boost: PAM3
C
Boost:
control
R848
IFN (U/ml)
Prime: HIV-GFP
Prime: cGAMP
- Vpx
+ Vpx
D
Boost:
control
R848
IFN (U/ml)
Prime:
mock
HIV-GFP +EFV
HIV-GFP +RAL
IN-D116A
ΔGag
LKO-GFP
E
Prime: cGAMP (μg/ml)
Boost: PAM3 (ug/ml)
IFNB1
IFNL1
CXCL10
IL1B
log2FC
F
IFN reporter
NF-κB reporter
IFN (U/ml)
NF-κB RLUs
mock
HIV-GFP
TNF
cGAMP
PAM3
R848
IFNa2a (U/ml)
IL-1β (ng/ml)
G
Prime:
mock
HIV-GFP
cGAMP (1 ug/ml)
IFN (U/ml)
Boost:
control
PAM3
R848
cGAMP (ug/ml)

Figure S4. Type I IFN responses triggered by HIV-GFP or cGAMP are boosted by unrelated innate stimuli. Related to Figure 4.

(A) Bioassay of type I IFN in supernatants from DCs that were primed for 28 h with HIV-GFP at an MOI of 0.5 or 1, then boosted with the indicated agonists overnight. Experiments were performed in parallel on DCs from 4 unique donors. Controls for agonist concentration = 0 (black circles) were performed once for each donor and plotted on each graph for reference.

(B) Flow cytometry of DCs stimulated as in (A), plotted as CD86 vs GFP. Plots are representative from 1 of 4 donors.

(C) DCs were treated with or without Vpx, then primed with either cGAMP or HIV-GFP as shown (Figure 4C, 4E), and then challenged with R848 (3 μg/ml) overnight. Graphs indicate bioactive type I IFN from DC supernatants. n = 4 donors.

(D) Type I IFN activity from DC supernatants that were primed for 28 h with HIV-GFP in the presence of EFV or RAL compared to IN-D116A, DeltaGag, or LKO-GFP, that were then treated with control (media) or boosted with R848 (3 μg/ml) overnight h. n = 5 donors.

(E). qPCR results plotted as heatmap of a prime-boost dose response matrix using cGAMP and PAM3. DCs were primed with 1 μg/ml 2,3-linked cGAMP for 7 h and boosted +/- PAM3 (100 ng/ml) for 1 h. Heatmaps represent qPCR data from 1 of 2 donors.

(F) The indicated stimuli on the x-axis were administered directly to type I IFN reporter cells or NF-κB reporter cells to determine (1) if these innate agonists could directly stimulate reporter activity, and (2) to evaluate the specificity of the reporter systems to distinguish IFN- and NF-κB-activating cytokines. Treatments were used at the following concentrations: HIV-GFP (MOI 15), TNFα (500 ng/ml), cGAMP (5 μg/ml), PAM3 (100 ng/ml), R848 (3 μg/ml), IFNa2a (as shown), and IL-1β (as shown). Reporter activity was scored after 7 h (see STAR METHODS).

(G) Bioactive type I IFN from DC supernatants after priming cells with HIV-GFP or cGAMP as indicated (Figure 4C, 4E) and then challenging with either PAM3 (100 ng/ml), R848 (3 μg/ml), or increasing doses of cGAMP. Data represent mean +/- SEM.

Figure S5

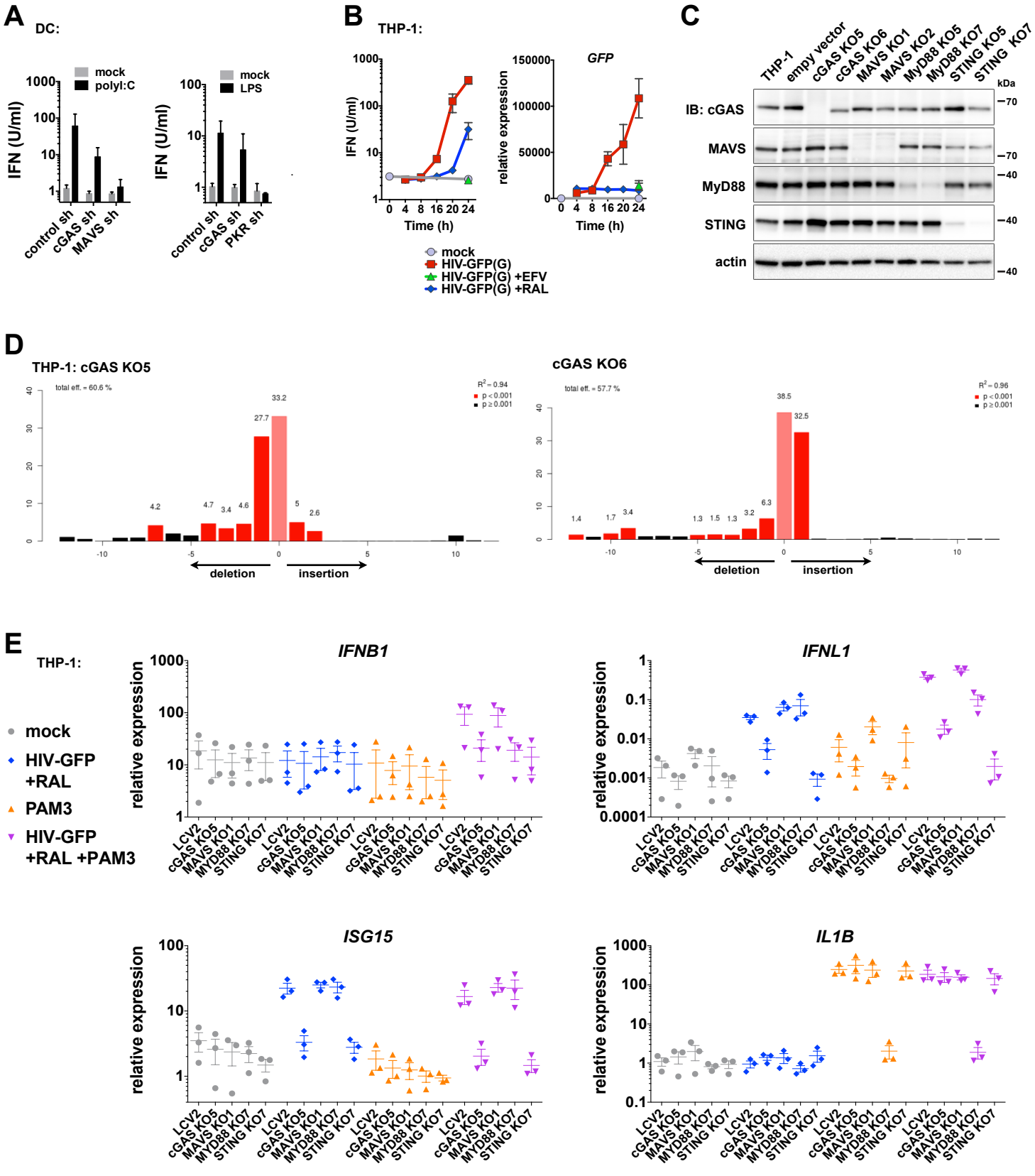
A
DC:
mock
polyI:C
IFN (U/ml)
control sh
cGAS sh
MAVS sh
mock
LPS
PKR sh
B
THP-1:
IFN (U/ml)
Time (h)
GFP
relative expression
mock
HIV-GFP(G)
HIV-GFP(G) +EFV
HIV-GFP(G) +RAL
C
THP-1
empy vector
cGAS KO5
cGAS KO6
MAVS KO1
MAVS KO2
MyD88 KO5
MyD88 KO7
STING KO5
STING KO7
kDa
IB: cGAS
MAVS
MyD88
STING
actin
D
THP-1: cGAS KO5
cGAS KO6
total eff. = 60.6 %
total eff. = 57.7 %
deletion
insertion
E
THP-1:
mock
HIV-GFP +RAL
PAM3
HIV-GFP +RAL +PAM3
IFNB1
IFNL1
ISG15
IL1B
relative expression
LCV2
cGAS KO5
MAVS KO1
MYD88 KO7
STING KO7

Figure S5. cGAS/STING and MYD88 are required for priming and boosting of IFN responses, respectively. Related to Figure 5.

(A) Bioactive type I IFN in supernatants from DCs transduced with shRNAs against the indicated targets that were transfected with polyI:C (100 ng/ml) or treated with LPS (1 ng/ml) for 16 h.

(B) Bioactive type I IFN and qPCR of *GFP* reporter expression in supernatants from THP-1 cells infected with HIV-GFP +/- EFV or RAL for the indicated times. n = 3.

(C) Immunoblots of lysates from THP-1 populations modified using the lentiCRISPR system. Two unique sgRNAs are shown for each target (cGAS, MAVS, MyD88, or STING), along with the vector control (LCV2).

(D) Tracking of Indels by Decomposition (TIDE) sequencing analysis of THP-1 cell pools transduced with lentiCRISPR clones cGAS KO5 and KO6 to assess target site perturbation prior to selection and population expansion. Red bars indicate indel formation as the percent of cells in the population containing insertions or deletions near the expected cut site. The anti-cGAS antibody used in panel (C) (Cell Signaling, Cat #15102S) is reported to bind an epitope surrounding Ala19 of cGAS, which is upstream of the region perturbed by CRISPR/Cas9 gRNA for cGAS KO6 (Arg28). Therefore, a perturbed cGAS or a frameshifted product generated from cGAS KO6 should still be detected by the anti-cGAS antibody, as seen for cGAS KO6 in panel (C) with a band migrating just below wild type.

(E) THP-1 CRISPR cells were primed with HIV-GFP+RAL or left unprimed (mock) for 28 h and then treated with vehicle or PAM3 (100ng/ml) for 1 h. Expression levels of *IFNB1, IFNL1, ISG15*, and *IL1B* were assessed by qPCR relative to *GAPDH*. n = 3.

Panels with pooled data show mean +/- SEM.

Figure S6

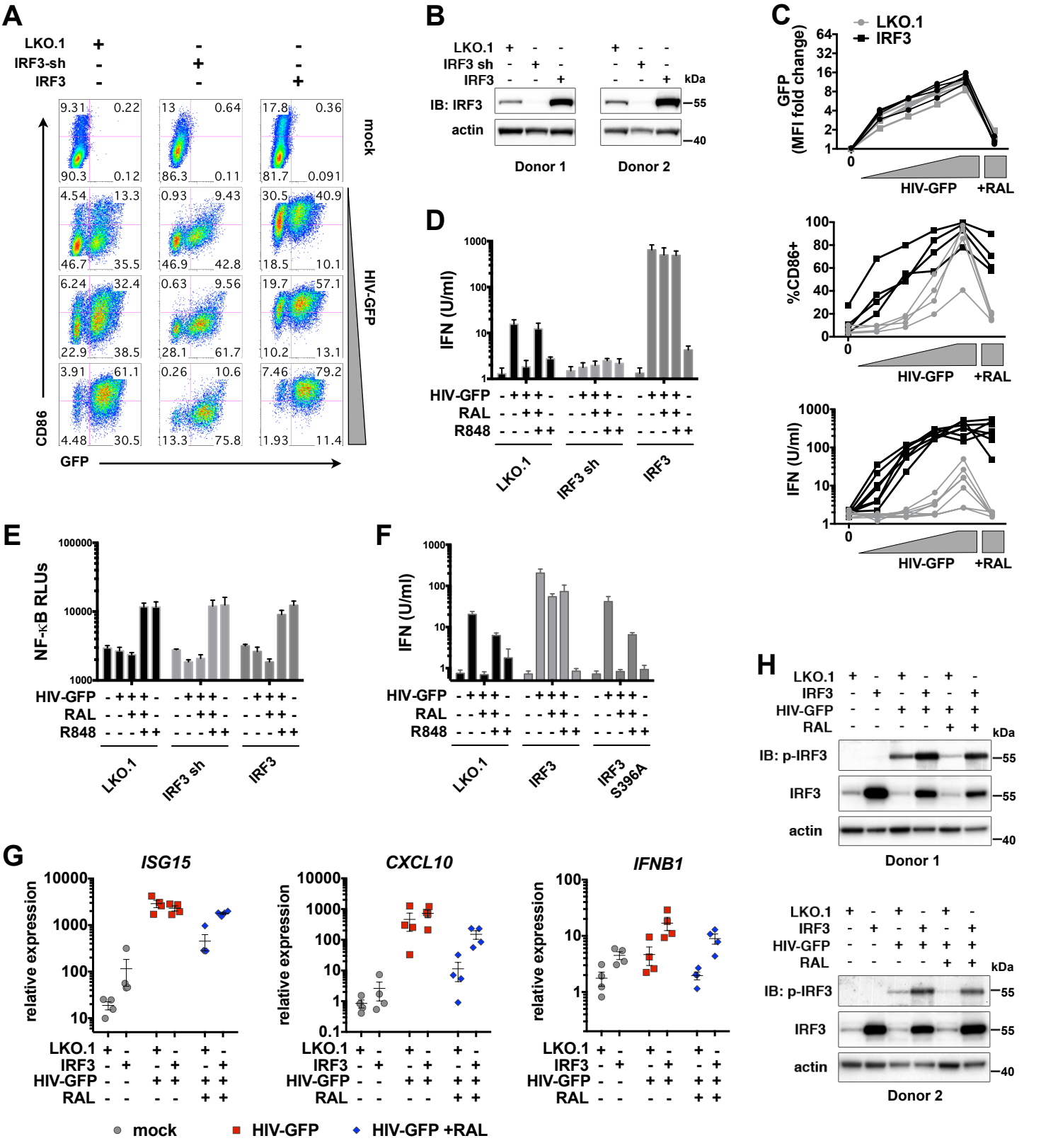
A
LKO.1
IRF3-sh
IRF3
mock
HIV-GFP
CD86
GFP
B
IB: IRF3
actin
kDa
Donor 1
Donor 2
C
LKO.1
IRF3
GFP (MFI fold change)
%CD86+
IFN (U/ml)
HIV-GFP
+RAL
D
IFN (U/ml)
RAL
R848
E
NF-κB RLUs
F
IFN (U/ml)
IRF3 S396A
G
ISG15
CXCL10
IFNB1
relative expression
mock
HIV-GFP
HIV-GFP +RAL
H
IB: p-IRF3
IRF3
actin
Donor 1
Donor 2

Figure S6. Availability of IRF3 sets the limit for HIV-mediated innate responses. Related to Figure 6.

(A) DCs were derived from CD14+ monocytes that were transduced with a control vector expressing puromycin (LKO.1), IRF3 shRNA, or an IRF3 overexpression vector. At day 4, DCs were challenged with HIV-GFP at MOIs of 0.5, 1.5, or 5 and analyzed by flow cytometry at 48 h to assess CD86 and GFP. Plots represent 1 of 4 donors.

(B) Immunoblots of DC whole cell lysates following transduction with LKO.1, IRF3 shRNA, or an IRF3 overexpression vector.

(C) Plots showing GFP, %CD86+, and bioactive type I IFN activity, 48 h after HIV-GFP infection at an MOI of 0.15, 0.5, 1.5, and 5 in DCs transduced with LKO.1 or a vector overexpressing IRF3. n = 4 donors (GFP and %CD86+) or 7 donors (IFN).

(D) Bioactive type I IFN activity from DC supernatants from indicated conditions after 48 h of stimulation. HIV-GFP MOI=5; R848 (3 μg/ml) was added 28 h after infection. n = 4 donors.

(E) NF-κB activity from supernatants of DCs treated under the conditions shown in (D). n = 4 donors.

(F) Bioactive type I IFN activity from supernatants of DCs treated under the conditions shown, similar to (D), comparing overexpression of IRF3 to the S396A mutation.

(G) qPCR of *ISG15, CXCL10*, and *IFNB1* expression from DCs infected with HIV-GFP under the conditions shown for 28 h.

(H) Immunoblots of whole cell lysates from DCs that had been transduced with a control vector (LKO.1) or an IRF3 overexpression vector which were challenged at day 4 with HIV-GFP +/- RAL for 24 h. Blots show levels of total and phosphorylated IRF3 (p-IRF3) under the conditions shown compared to actin controls.

Panels with pooled data show mean +/- SEM.

Figure S7

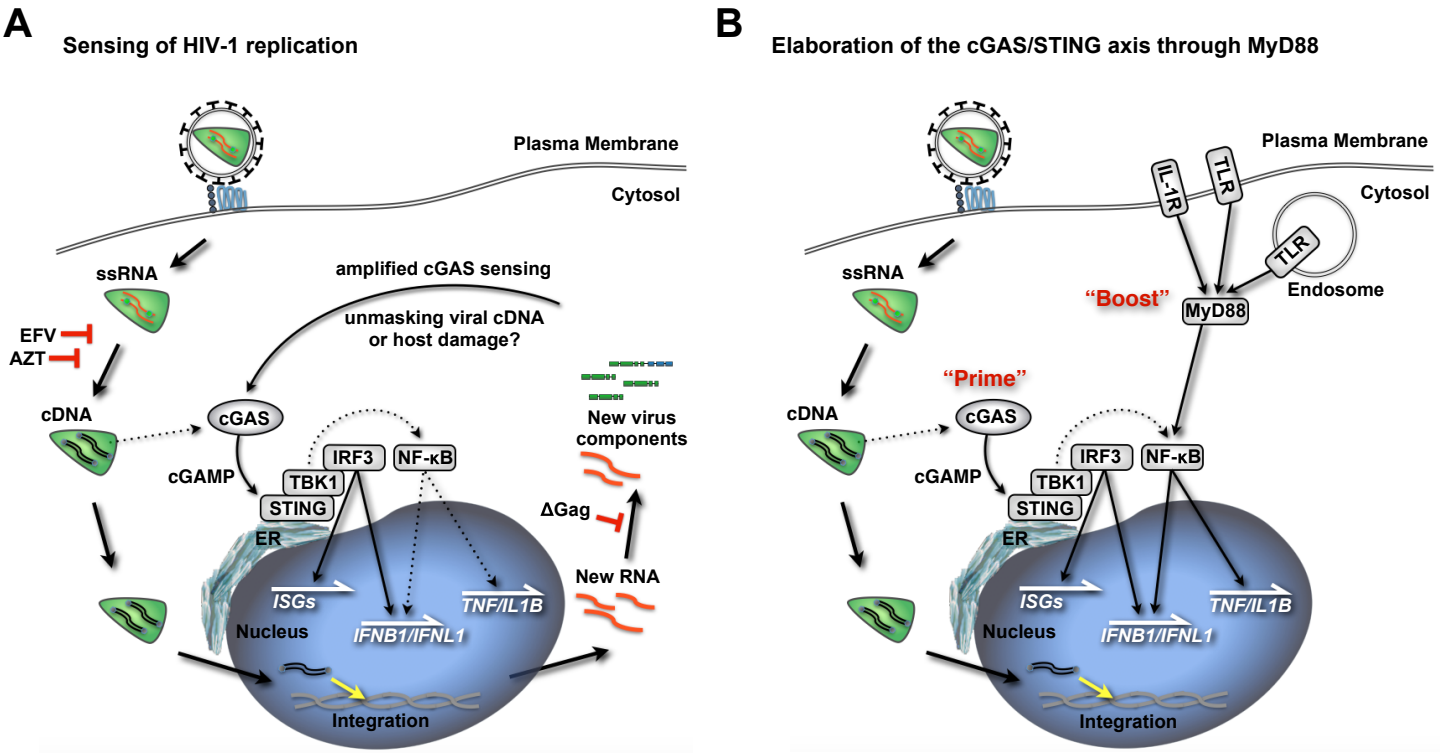
A
Sensing of HIV-1 replication
Plasma Membrane
Cytosol
ssRNA
amplified cGAS sensing
unmasking viral cDNA
or host damage?
EFV
AZT
cDNA
cGAS
New virus
components
cGAMP
IRF3
NF-κB
TBK1
STING
ΔGag
ER
New RNA
ISGs
TNF/IL1B
Nucleus
IFNB1/IFNL1
Integration
B
Elaboration of the cGAS/STING axis through MyD88
Plasma Membrane
IL-1R
TLR
Cytosol
TLR
Endosome
ssRNA
"Boost"
MyD88
"Prime"
cDNA
cGAS
cGAMP
IRF3
NF-κB
TBK1
STING
ER
ISGs
TNF/IL1B
Nucleus
IFNB1/IFNL1
Integration

Figure S7. Model for how HIV replication and MyD88 stimulation elaborate STING-mediated IFN responses. Related to Figure 7.

(A) HIV cDNA is inefficiently detected by cGAS during entry. Replication of virus increases this response by either unmasking preexisting cDNA, triggering collateral host damage that is sensed by cGAS, or a combination thereof.

(B) Low IFN responses driven by the cGAS/STING axis (either during HIV infection or exogenous cGAMP administration) can be enhanced by stimulation through unrelated pathways, such as those activating MyD88.